

Long-Lived Double-Barred Galaxies From Pseudo-Bulges

Victor P. Debattista¹

Astronomy Department, University of Washington, Box 351580, Seattle, WA 98195

and

Juntai Shen²

*McDonald Observatory, The University of Texas at Austin, 1 University Station, C1402,
Austin, TX 78712*

ABSTRACT

A large fraction of barred galaxies host secondary bars that are embedded in their large-scale primary counterparts. These are common also in gas poor early-type barred galaxies. The evolution of such double-barred galaxies is still not well understood, partly because of a lack of realistic N -body models with which to study them. Here we report a new mechanism for generating such systems, namely the presence of rotating pseudo-bulges. We demonstrate with high mass and force resolution collisionless N -body simulations that long-lived secondary bars can form spontaneously without requiring gas, contrary to previous claims. We find that secondary bars rotate faster than primary ones. The rotation is not, however, rigid: the secondary bars pulsate, with their amplitude and pattern speed oscillating as they rotate through the primary bars. This self-consistent study supports previous work based on orbital analysis in the potential of two rigidly rotating bars. The pulsating nature of secondary bars may have important implications for understanding the central region of double-barred galaxies.

Subject headings: stellar dynamics — galaxies: bulges — galaxies: evolution — galaxies: formation — galaxies: kinematics and dynamics — galaxies: structure

¹Brooks Prize Fellow; email: debattis@astro.washington.edu

²Harlan J. Smith Fellow; email: shen@astro.as.utexas.edu

1. Introduction

Double-barred (S2B) galaxies, consisting of a small scale nuclear/secondary bar (B2) embedded within a large scale primary bar (B1), have been known for over thirty years (e.g. de Vaucouleurs 1975). Erwin & Sparke (2002) carefully compiled statistics for early-type optically-barred galaxies from images by both the WIYN telescope and the *Hubble Space Telescope*, and concluded that at least one quarter of them are double-barred. The facts that inner bars are also seen in near-infrared (e.g. Mulchaey et al. 1997; Laine et al. 2002), and that gas-poor S0s often contain inner bars indicate that most of them are stellar structures. S2Bs may play an important role in the formation and nurture of supermassive black holes (SMBHs). S2B galaxies have been hypothesized to be a possible mechanism for driving gas past the inner Lindblad resonance of B1s, feeding SMBHs and powering AGN (Shlosman et al. 1989). S2Bs have also been suggested as a mechanism for forming SMBHs directly (Begelman et al. 2006).

Such fueling requires that the B2 and the B1 are dynamically decoupled.³ The random apparent orientations of B1s and B2s in nearly face-on galaxies points to dynamical decoupling (Buta & Crocker 1993; Friedli & Martinet 1993). But images alone cannot reveal how the two bars rotate through each other. Kinematic evidence of decoupling, using either gas or stars, is harder to obtain (Petitpas & Wilson 2002; Schinnerer et al. 2002; Moiseev et al. 2004). Indirect evidence for decoupling was suggested by Emsellem et al. (2001) based on rotation velocity peaks inside the B2s in three S2B galaxies. Conclusive direct kinematic evidence for a decoupled B2 was obtained for NGC 2950 by Corsini et al. (2003) who showed, using the method of Tremaine & Weinberg (1984), that its B1 and B2 cannot be rotating at the same rate.

An important advance in understanding S2B galaxies came from the development by Maciejewski & Sparke (1997, 2000, hereafter MS00) of the formalism necessary for studying their orbits. They introduced the concept of loops, families of orbits in which particles return to the same curve, but not the same position, after the two bars return to the same relative orientation. MS00 considered two models assuming that the B2 is more rapidly rotating than the B1: the B2 in their Model 1 ended near its corotation radius, while in their Model 2 it ended well inside this radius. MS00 were unable to find loop orbits supporting the outer parts of the B2 in Model 1 but succeeded in doing so in the more slowly rotating Model 2. Using hydrodynamical simulations of such slowly rotating rigid B2s Maciejewski et al. (2002) found them to be inefficient at driving gas to small radii.

³In this context, by decoupled we mean only that $\Omega_{B2} \neq \Omega_{B1}$, where Ω_{B2} (Ω_{B1}) is the pattern speed of the B2 (B1).

Such models are not fully self-consistent since, in general, nested bars cannot rotate rigidly through each other (Louis & Gerhard 1988). In fact non-solid body rotation was hinted at by the loop orbit calculations of MS00. N -body simulations provide one route to more self-consistent models of S2Bs, but until now there existed a paucity of such models. Most numerical studies (e.g. Shlosman & Heller 2002; Friedli & Martinet 1993; Englmaier & Shlosman 2004) required gas to form B2s; for example, Heller et al. (2001) formed them via viscosity-driven instabilities in nuclear gas rings, which lead to B2s rotating slower than B1s. But the presence of B2s in a large fraction of gas-poor early-type galaxies (Erwin & Sparke 2002; Petitpas & Wilson 2002) indicates that B2s are not an exclusively gas dynamical phenomenon. Counter-rotation in stellar disks can lead to decoupled counter-rotating bars (Sellwood & Merritt 1994; Friedli 1996; Davies & Hunter 1997), but such counter-rotation is infrequent (Kuijken et al. 1996). Only Rautiainen and collaborators (Rautiainen & Salo 1999; Rautiainen et al. 2002) have succeeded in forming long-lived B2s rotating in the same sense as the B1 in purely collisionless studies. The mechanism by which the B2s formed in these however simulations remains unclear.

In light of the increasing evidence that SMBH feedback may play an important role in galaxy formation (Springel et al. 2005) and the possibility that S2Bs may provoke AGNs, the paucity of self-consistent N -body models of S2Bs is a major hindrance to further theoretical development. The time is ripe, therefore, to examine whether unambiguous and independently rotating nested bars can form in high resolution collisionless simulations. Kormendy & Kennicutt (2004) pointed out that a nuclear bar constitutes strong evidence of a pseudo-bulge, i.e., a bulge with a disky character. Such pseudo-bulges form through the secular evolution of disks, via both gas and stellar dynamical processes (see the review of Kormendy & Kennicutt 2004). One of the main characteristics of pseudo-bulges is that they rotate rapidly, a property which favors them to become bar unstable. In this work, we demonstrate that a rapidly rotating bulge can develop a long-lived B2 in collisionless N -body simulations.

2. Model Setup

We focus on two examples of simulations which formed long-lasting double-barred systems taken from a large survey of such simulations. Our high-resolution simulations consist of live disk and bulge components in a rigid halo potential. We restrict ourselves to rigid halos to afford high mass resolution in the nuclear regions, to study the complicated co-evolution of the two bars without the additional evolution introduced by the halo, and to compare with the models of MS00. We defer the study of S2B systems in live halos to a future publication.

The rigid halos used in this study are all logarithmic potentials $\Phi(r) = \frac{1}{2}V_h^2 \ln(r^2 + r_h^2)$. We set $V_h = 0.6$ in both runs and $r_h = 15$ in run 1 and $r_h = 10$ in run 2. Both initial disks in our simulations have exponential surface densities with scale-length R_d , mass M_d and Toomre- $Q \simeq 2$. The bulge was generated using the method of Prendergast & Toomer (1970) as described in Debattista & Sellwood (2000), where a distribution function is integrated iteratively in the global potential, until convergence. In both cases the bulge has mass $M_b = 0.2M_d$ and we used an isotropic King model distribution function. The bulge truncation radius is $0.7R_d$ in run 1 and $1.0R_d$ in run 2. The bulge set up this way is non-rotating. We introduce bulge rotation by simply reversing the velocities of bulge particles with negative angular momenta, which is still a valid solution of the collisionless Boltzmann equation (Lynden-Bell 1962). The bulge in run 1 is flattened by the disk potential to an edge-on projected ellipticity of $\epsilon_b \simeq 0.25$. The ratio $V_p/\bar{\sigma} \simeq 0.8$, where V_p is the peak velocity and $\bar{\sigma}$ is the average velocity dispersion inside the half mass radius. In run 2, the corresponding values are $\epsilon_b \simeq 0.38$ and $V_p/\bar{\sigma} \simeq 0.7$. The kinematic values relative to the oblate isotropic rotators are $(V_p/\bar{\sigma})_* \simeq 1.3$ for run 1 and $(V_p/\bar{\sigma})_* \simeq 0.9$ for run 2. Thus both pseudo-bulges are above or close to the locus of oblate isotropic rotators. These pseudo-bulges are less tangentially biased and more pressure supported than rotationally-supported pseudo-bulges which would form out of gas driven to small radii. Our simulations therefore probably under-estimate the tendency for pseudo-bulges to form nuclear bars.

We use R_d and M_d as the units of length and mass, respectively, and the time unit is $(R_d^3/GM_d)^{1/2}$. If we scale these units to the physical values $M_d = 2.3 \times 10^{10}M_\odot$ and $R_d = 2.5$ kpc, then a unit of time is 12.3 Myr. We use a force resolution (softening) of 0.01, which scaled to the above physical units corresponds to 25 pc. Both models had 1.2×10^6 equal mass particles, with 10^6 in the disk. These simulations were evolved with a 3-D cylindrical polar grid code (Sellwood & Valluri 1997). This code expands the potential in a Fourier series in the cylindrical polar angle ϕ ; we truncated the expansion at $m = 8$. Forces in the radial direction are solved for by direct convolution with the Greens function while the vertical forces are obtained by fast Fourier transform. We used grids measuring $N_R \times N_\phi \times N_z = 58 \times 64 \times 375$. The vertical spacing of the grid planes was $\delta z = 0.01R_d$. Time integration used a leapfrog integrator with a fixed time-step $\delta t = 0.04$.

3. Results

Figure 1 gives a general view of the evolution of run 1 over 750 time units (~ 9.2 Gyr in our standard scaling). A nuclear bar forms rapidly (before $t = 10$), as the dynamical times in the inner galaxy are much shorter than in the outer part. The pattern speed, Ω_{B2} , of

this nuclear bar is large at this stage, and it extends to nearly its corotation radius, $R_{c,B2}$, indicating that it forms by the usual bar instability (Toomre 1981). The B1 forms at a later stage, between $t = 100$ and 200. The evolution of the amplitudes of the B1 and B2 (A_{B1} and A_{B2} respectively), defined as the Fourier $m = 2$ amplitude over the radial ranges $0.5 \leq R \leq 2$ and $R \leq 0.3$, is shown in the left panel of Figure 2. The B2 is strong initially, but it weakens once the B1 forms. At the same time Ω_{B2} also decreases and, since its semi-major axis does not change substantially, it no longer extends to $R_{c,B2}$. The transition to a stable S2B state is accomplished during a seemingly chaotic period during which both bars undergo phases when they are rather weak. After $t = 250$, however, the B2 settles into an oscillatory steady state with A_{B2} exhibiting regular oscillations. The double-barred state persists to the end of the simulation, lasting for ~ 7 Gyr. The B2 shows up in both the disk and bulge particles.

The B2 is stronger when the bars are perpendicular, and weaker when they are parallel to each other (Figure 2). Note that this behavior is exactly opposite to the variations of gaseous rings in Heller et al. (2001). The amplitude of the primary bar instead varies in the opposite sense with respect to the relative phase of the two bars, although the amplitude of this oscillation is smaller. A_{B1} also decreases slowly after $t = 250$, possibly because orbits supporting the B1 are gradually disrupted by the relatively strong inner bar. As a consequence, the oscillations in A_{B2} decrease as the B1 weakens.

The right panel of Figure 2 shows the evolution of A_{B1} and A_{B2} in run 2. The main difference between run 2 and run 1 is that the initial bulge is larger in run 2, allowing the B2 to dominate the global dynamics. As a result, the B1 oscillates more strongly than the B2. This probably represents an extreme case of the dynamical influence of a B2 on a B1.

The long-lived B2 rotates faster than the B1: between $t = 300$ and $t = 400$ the average rotation period of the B2 in run 1 is about $\tau_{B2} \simeq 17.6$, and for the B1 $\tau_{B1} \simeq 27.8$. The pattern speed of the B2, Ω_{B2} , also varies with the relative phase of the two bars: it is larger when the two bars align, and smaller when they are orthogonal. We plot in Figure 3 the system in the corotating frame of the B1. The variations of both A_{B2} and Ω_{B2} are readily visible. The variation of Ω_{B2} can be $> 20\%$ but is much less significant for Ω_{B1} (Figure 4). Defining $\langle \Omega_{B2} \rangle$ ($\langle \Omega_{B1} \rangle$) as the average pattern speed of the B2 (B1) over one relative rotation, we plot in the inset of Figure 4 the phase difference between $\langle \Omega_{B2} \rangle t$ ($\langle \Omega_{B1} \rangle t$) and the phase of the B2 (B1). The B1 is seen to rotate with a rather constant Ω_{B1} but the B2 experiences a large variation in Ω_{B2} over one relative rotation.

Figure 5 presents ellipse fits using IRAF for times when the B2 and B1 are perpendicular and at $\sim 45^\circ$ to each other. In both cases the phase of the B2 is constant to within 10° and there is little sense of spirality in it. This is distinctly a nuclear bar rather than a nuclear spiral.

We measured the sizes of the two bars, for two different relative orientations at $t = 340$ and at $t = 350$, as the larger radius where the bar phase deviates by more than 10° from a constant value. We find a semi-major axis ratio $\simeq 0.10$ ($\simeq 0.12$) at $t = 340$ ($t = 350$), in good agreement with the typical size ratio of local S2B systems (Erwin & Sparke 2002).

4. Discussion and Conclusions

Our self-consistent simulations of S2B systems can be compared to the models of MS00. The simulations all exhibited oscillating pattern speeds and amplitudes for one or both bars. Similarly MS00 found that the x_2 loops supporting the B2 change axis ratios and lead or trail the rigid figure of the B2, as the bars rotate. The loop orbits of MS00 were more elongated in the B2 region when the two bars were orthogonal than when they were parallel. The pulsating character of the self-consistent B2 in the simulations provides strong evidence that x_2 loops are the backbone of the double bars in these simulations. This behavior is also in good agreement with the earlier prediction by Louis & Gerhard (1988) that independent rigid rotation of two bars is not possible. The x_2 loop orbits of MS00 also suggested that Ω_{B2} would be largest when the two bars are parallel, which is also borne out by the simulations. Furthermore, MS00 were unable to find supporting x_2 orbits when the B2 extended to about $R_{c,B2}$, while we found that Ω_{B2} had to decrease once the B1 formed and the B2 did not extend to $R_{c,B2}$, again in good agreement with MS00. Our simulations also suggest that observationally there should be a slight excess of close-to-perpendicular double bars, as the secondary bar tends to rotate slower when two bars are perpendicular.

The main objective of this work is to create S2B systems and show how the two bars form spontaneously, interact and evolve. Our simulations all form B2s before they form B1s. However this is not a prediction of our model and it occurs only because, for simplicity, we introduced our rotating pseudo-bulge from $t = 0$. It is more likely that a pseudo-bulge would form after gas is driven to the center by a pre-existing B1. Our pseudo-bulges all had rotation; B2s did not form in simulations without pseudo-bulge rotation (these results will be presented elsewhere, but see for example Debattista 2003). In contrast, Rautiainen & Salo (1999) produced B2s even though their bulges were analytic.

We are able to form well-resolved, long-lived B2s in purely collisionless N -body simulations. The nuclear bars are distinctly barred, not spiral, and reach to the center. These simulations demonstrate that B2s do not need to be gaseous. We confirm that pseudo-bulge rotation may be an important ingredient for the formation of double-barred galaxies (Kormendy & Kennicutt 2004). The required degree of rotation is modest and not greater than that associated with pseudo-bulges (Kormendy 1993). The B2s in these simulations rotate

faster than the B1s. The implications of the pulsating nature of B1s on central gas inflow are unclear at present. This new method for forming S2B models reliably and repeatedly should prove a boon to exploring their dynamics and evolution, their observational properties, their effect on gas, etc. We will report on these issues elsewhere.

V.P.D. is supported by a Brooks Prize Fellowship at the University of Washington and receives partial support from NSF ITR grant PHY-0205413. V.P.D. thanks the University of Texas at Austin for hospitality during part of this project.

REFERENCES

- Begelman, M. C., Volonteri, M., & Rees, M. J. 2006, astro-ph/0602363
- Buta, R., & Crocker, D. A. 1993, AJ, 105, 1344
- Corsini, E. M., Debattista, V. P., & Aguerri, J. A. L. 2003, ApJ, 599, L29
- Davies, C. L., & Hunter, J. H. 1997, ApJ, 484, 79
- de Vaucouleurs, G. 1975, ApJS, 29, 193
- Debattista, V. P. 2003, MNRAS, 342, 1194
- Debattista, V. P., & Sellwood, J. A. 2000, ApJ, 543, 704
- Emsellem, E., Greusard, D., Combes, F., Friedli, D., Leon, S., Pécontal, E., & Wozniak, H. 2001, A&A, 368, 52
- Englmaier, P., & Shlosman, I. 2004, ApJ, 617, L115
- Erwin, P. 2004, A&A, 415, 941
- Erwin, P., & Sparke, L. S. 2002, AJ, 124, 65
- Friedli, D. 1996, A&A, 312, 761
- Friedli, D., & Martinet, L. 1993, A&A, 277, 27
- Heller, C., Shlosman, I., & Englmaier, P. 2001, ApJ, 553, 661
- Kormendy, J. 1993, in IAU Symp. 153: Galactic Bulges, ed. H. Dejonghe & H. J. Habing, 209

- Kormendy, J., & Kennicutt, R. C. 2004, *ARA&A*, 42, 603
- Kuijken, K., Fisher, D., & Merrifield, M. R. 1996, *MNRAS*, 283, 543
- Laine, S., Shlosman, I., Knapen, J. H., & Peletier, R. F. 2002, *ApJ*, 567, 97
- Louis, P. D., & Gerhard, O. E. 1988, *MNRAS*, 233, 337
- Lynden-Bell, D. 1962, *MNRAS*, 123, 447
- Maciejewski, W., & Sparke, L. S. 1997, *ApJ*, 484, L117
- Maciejewski, W., & Sparke, L. S. 2000, *MNRAS*, 313, 745
- Maciejewski, W., Teuben, P. J., Sparke, L. S., & Stone, J. M. 2002, *MNRAS*, 329, 502
- Moiseev, A. V., Valdés, J. R., & Chavushyan, V. H. 2004, *A&A*, 421, 433
- Mulchaey, J. S., Regan, M. W., & Kundu, A. 1997, *ApJS*, 110, 299
- Petitpas, G. R., & Wilson, C. D. 2002, *ApJ*, 575, 814
- Prendergast, K. H., & Tomer, E. 1970, *AJ*, 75, 674
- Rautiainen, P., & Salo, H. 1999, *A&A*, 348, 737
- Rautiainen, P., Salo, H., & Laurikainen, E. 2002, *MNRAS*, 337, 1233
- Schinnerer, E., Maciejewski, W., Scoville, N., & Moustakas, L. A. 2002, *ApJ*, 575, 826
- Sellwood, J. A., & Merritt, D. 1994, *ApJ*, 425, 530
- Sellwood, J. A., & Valluri, M. 1997, *MNRAS*, 287, 124
- Shlosman, I., Frank, J., & Begelman, M. C. 1989, *Nature*, 338, 45
- Shlosman, I., & Heller, C. H. 2002, *ApJ*, 565, 921
- Silverman, B. W. 1986, *Density estimation for statistics and data analysis* (Monographs on Statistics and Applied Probability, London: Chapman and Hall)
- Springel, V., Di Matteo, T., & Hernquist, L. 2005, *MNRAS*, 361, 776
- Toomre, A. 1981, in *Structure and Evolution of Normal Galaxies*, ed. S. M., Fall & D. Lynden-Bell (Cambridge: Cambridge University Press), 111
- Tremaine, S., & Weinberg, M. D. 1984, *ApJ*, 282, L5

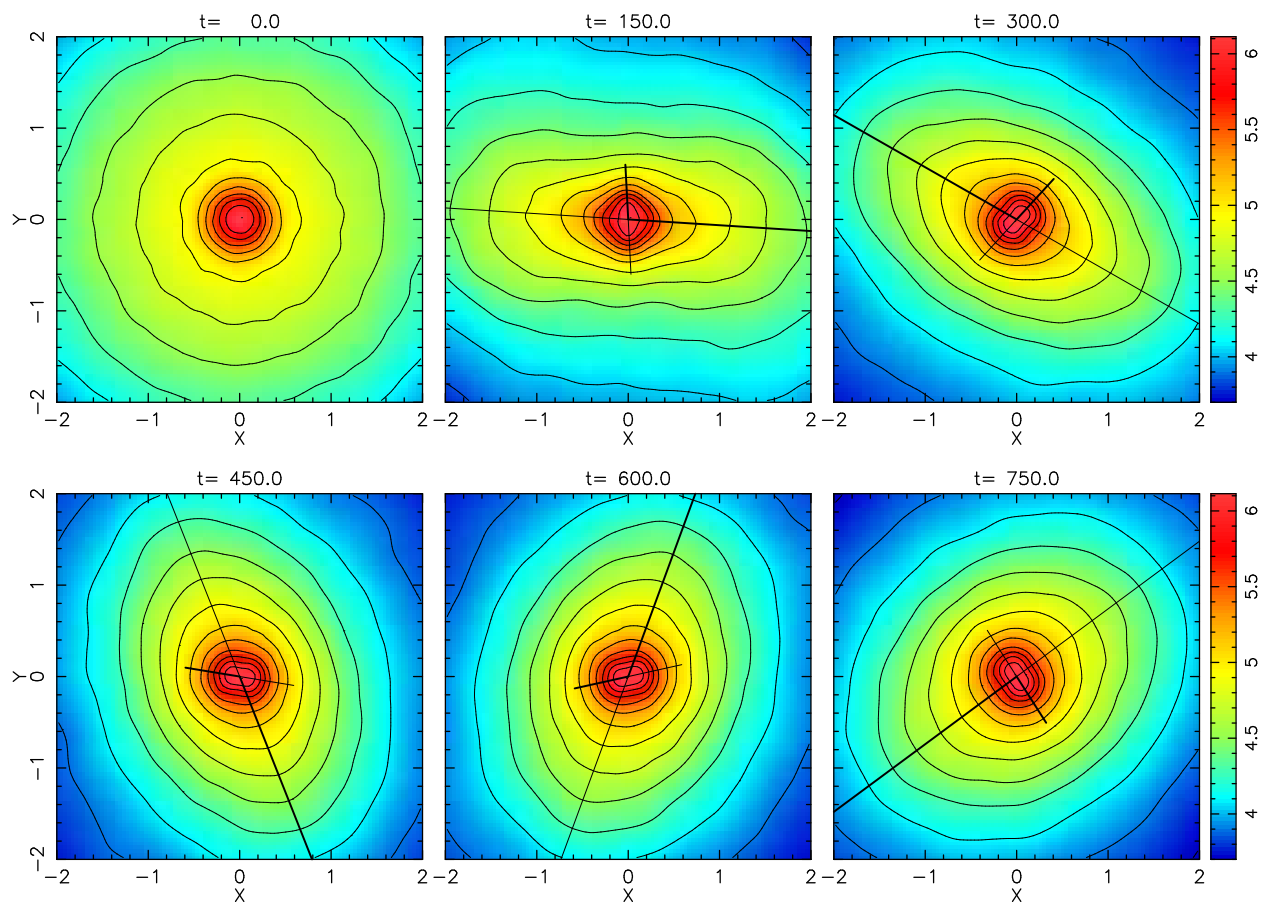


Fig. 1.— Images of total stellar distribution at various times, with iso-density contours superposed. The contours are logarithmic and separated by 0.2 dex. The heavy short and long straight lines mark the major axes of the B2 and B1, respectively. The surface density is obtained by smoothing every particle with an adaptive kernel (Silverman 1986). Note that 100 time units is about 1.2 Gyr, and the length unit is the scale-length of the initial disk.

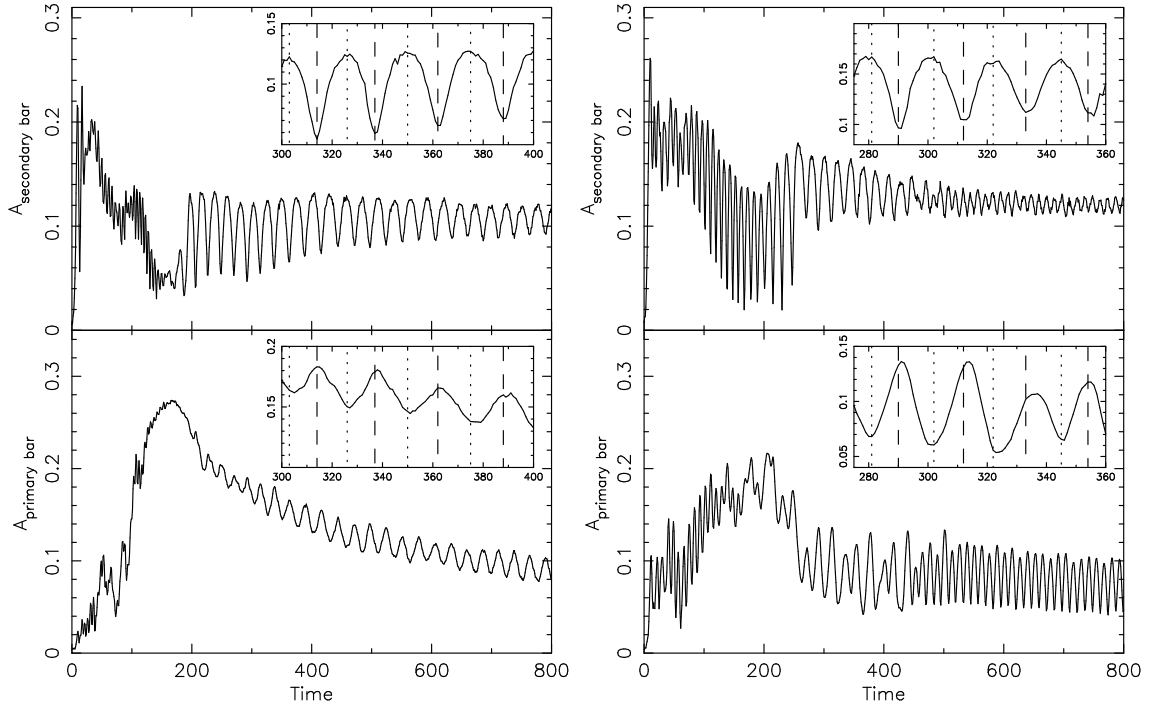


Fig. 2.— The time evolution of the bar amplitude of the B2 (*top panels*) and the B1 (*bottom panels*). In the insets, the dashed lines mark times when the two bars nearly align, while the dotted lines mark the time when they are perpendicular to each other. The beat period $\tau_{\text{beat}} = \tau_{\text{B1}}\tau_{\text{B2}}/2(\tau_{\text{B1}} - \tau_{\text{B2}})$. Run 1 is shown on the left, while run 2 is on the right.

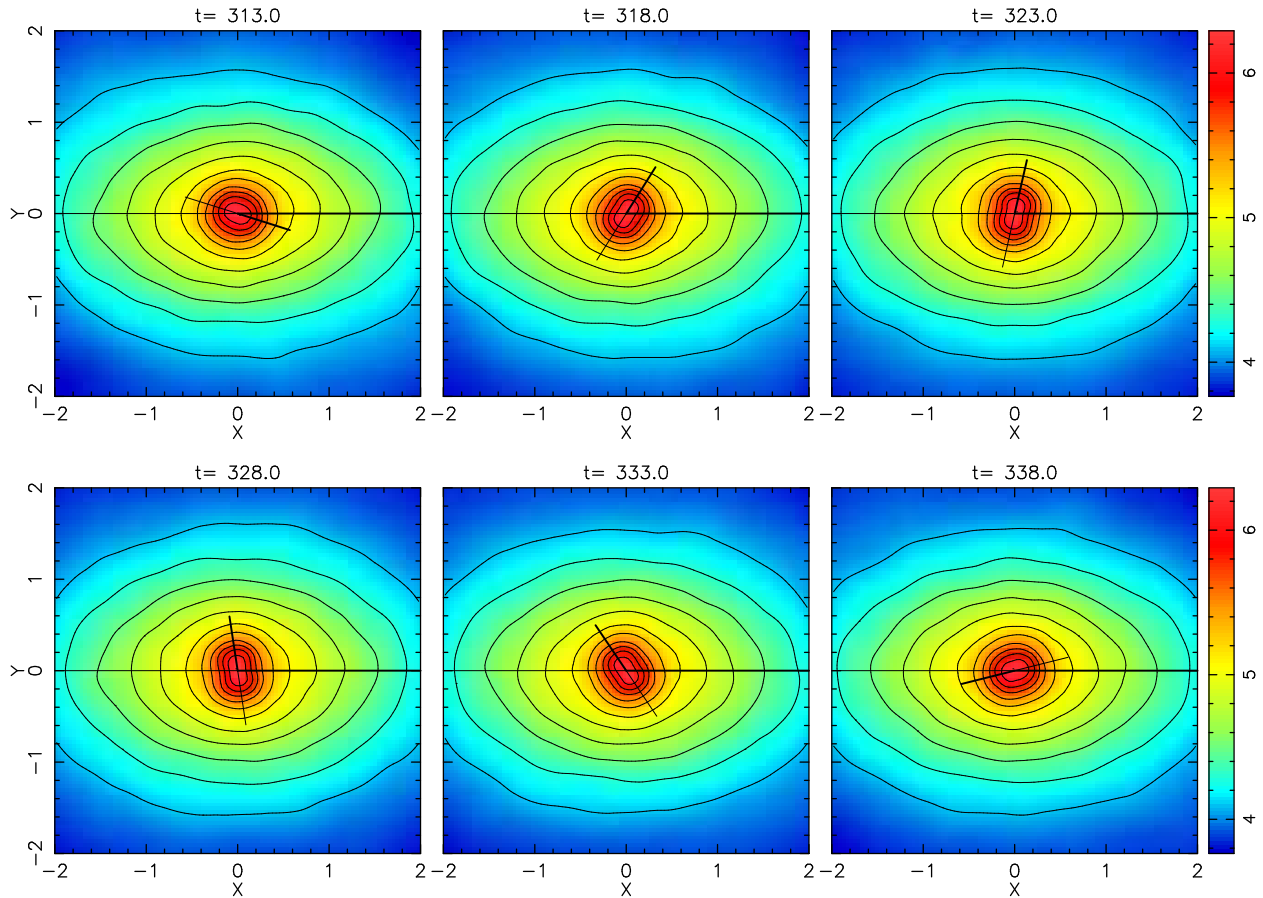


Fig. 3.— The non-uniform relative rotation of the B2 for roughly half of a period, in the corotating frame of the B1 which remains horizontal. The panels are equally-spaced in time. The straight line marks the major axis of the B2. The B2 rotates faster when the two bars align than when the two bars are perpendicular.

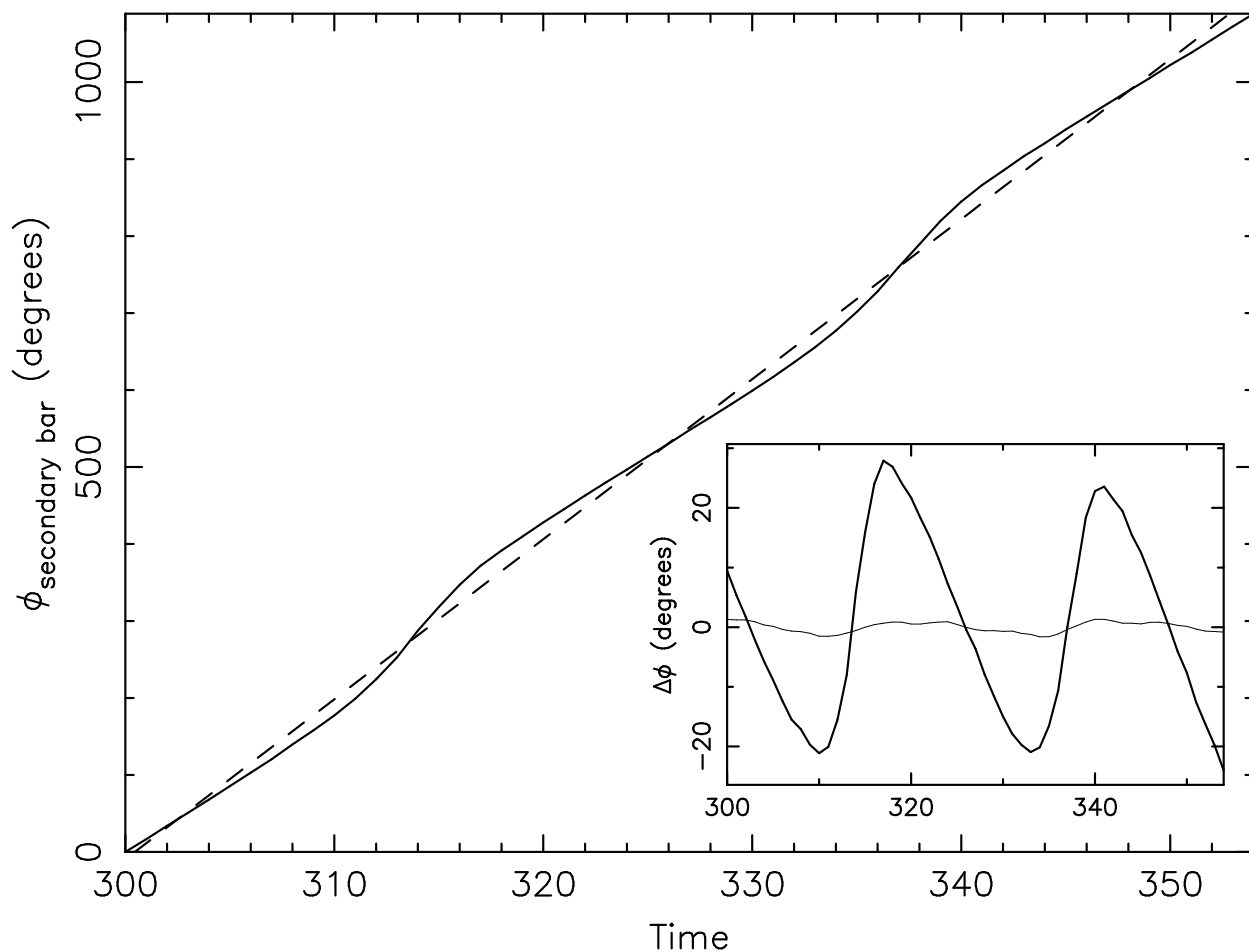


Fig. 4.— The time evolution of the phase of the B2, measured relative to $t = 300$. The dashed straight line is the least-square fit which gives the slope $\langle \Omega_{B2} \rangle$. The inset figure shows the phase difference, $\Delta\phi$ between the phases of the bars and $\langle \Omega \rangle t$, where $\langle \Omega \rangle$ is the pattern speed averaged over one relative rotation of the two bars; the thick line is for the B2 while the thin line is for the B1.

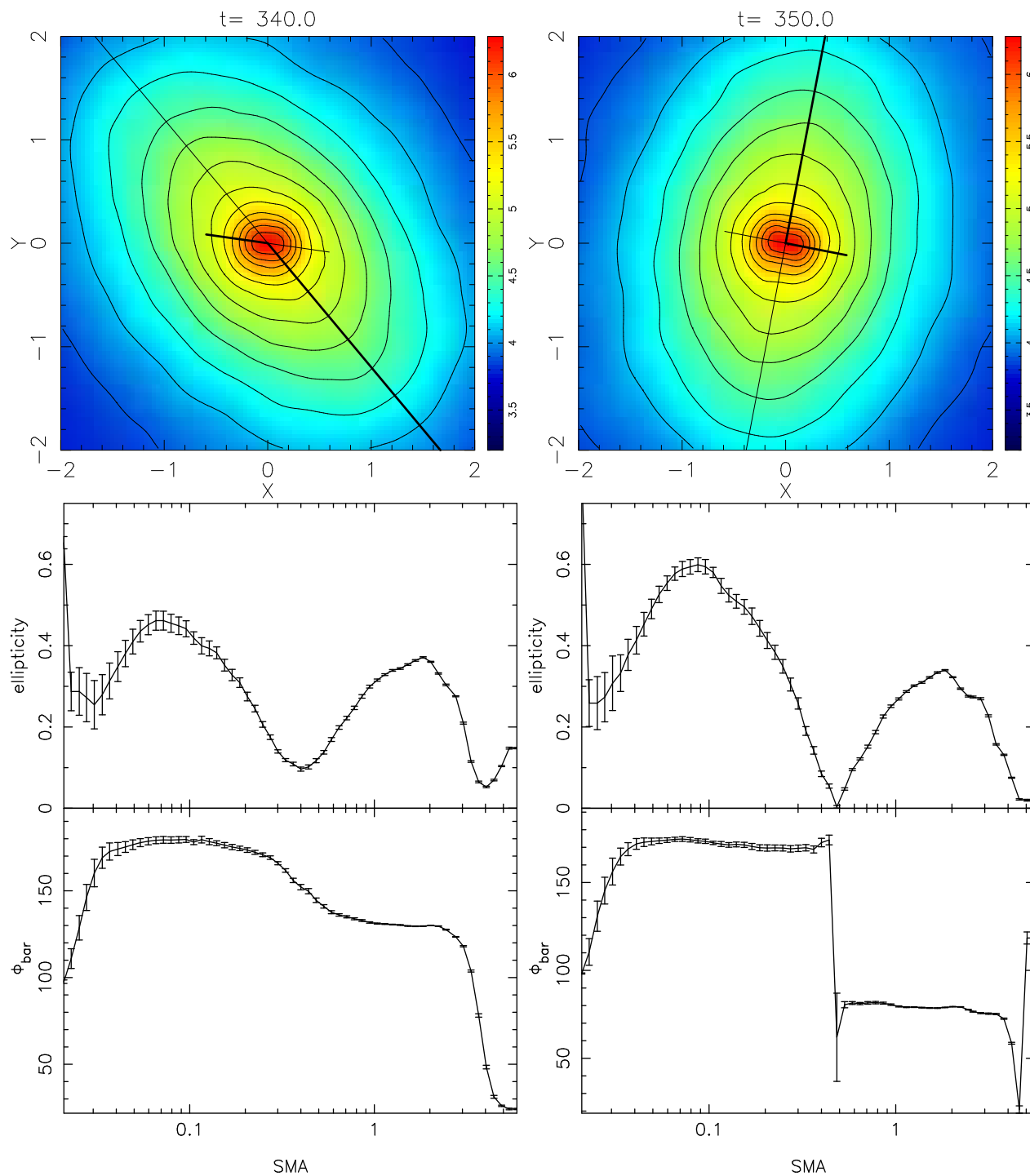


Fig. 5.— Results of ellipse fits using IRAF. Top panels: snapshots of run 1 at $t = 340$ (left) and $t = 350$ (right). The two bars are at $\sim 45^\circ$ at $t = 340$ and perpendicular at $t = 350$. Middle panels: Ellipticity as a function of semi-major axis (SMA) of fitted ellipses. Bottom panels: Position angle as a function of SMA of fitted ellipses.